CNRS
Centre National de la Recherche Scientifique

INFN
Istituto Nazionale di Fisica Nucleare

Design of the last stage of laser frequency stabilisation and laser frequency noise requirements

François BONDU

* * *

VIR-NOT-OCA-1390-227
Issue: 1
Date : December 5, 2002

VIRGO * A joint CNRS-INFN Project
Project Office: Traversa H di Via Macerata, I-56021 S. Stefano a Macerata (Pisa)
Secretariat: Telephone (39) 050 752 511 * FAX (39) 050 752 550 * e-mail W3@virgo.infn.it

1 Introduction

The Virgo interferometer needs a stabilisation of the laser frequency noise that uses the common mode of the 3-km long Fabry-Perot cavities [1]. Indeed, the dark fringe port is sensitive to both gravitational wave strain and laser frequency noise:

$$s_{\rm D1} = \alpha(h + \beta\frac{\delta\tilde{\nu}}{\nu_0}) \tag{1}$$

where α is a constant, h is the gravitational wave strain, β the interferometer effective asymmetry to laser frequency noise (a few %), $\delta\tilde{\nu}$ is the remaining laser frequency noise and $\nu_0 = c/\lambda$ is the light frequency. Hence, to detect a few $10^{-23}/\sqrt{\rm Hz}$, one needs a laser frequency stable at the few $10^{-7}{\rm Hz}/\sqrt{\rm Hz}$ level.

The amount of tolerated remaining laser frequency noise depends on $\nu_{\rm las}$, the laser frequency noise at the output of mode cleaner, and of the open loop transfer function $G_{\rm CM}$ of the last stage of frequency stabilisation (the "common mode"):

$$\delta\tilde{\nu} = \frac{\nu_{\rm las}}{1 + G_{\rm CM}} \tag{2}$$

So the requirements on the pre-stabilized laser frequency noise depends on the design of the common mode servo loop.

Up to now, the requirement on the laser frequency noise depends on a rough estimation of the response of the interferometer to laser frequency noise [1, 2, 3]. The unity gain for the last stage of frequency stabilisation was supposed to be one third of the long arm free spectral range, and the slope of the open loop transfer function assumed to be $f^{-1.5}$ at unity gain. Actually, it was suspected that "something wrong" happens in the transfer function for frequencies close to the free spectral range, but it was not clear what to expect. The exact shape of the response of the full interferometer to the frequency noise is required to design the corrector filter with precise knowledge of gain and phase margin.

The second section of this note describes how to obtain precise transfer functions using the JAJY program. It then shows how to deduce the requirement on the laser frequency noise using a set of four transfer functions and the design of the common mode servo loop. The third section applies the equations of the second section to the case where the light used to sense the common mode of the long arms is the one reflected by the AR coated face of the beamsplitter, on photodiode D5, demodulated at 6 MHz. The fourth section is the same application where the sensing of the common mode of the interferometer is done on the light reflected by the interferometer (photodiode D2), demodulated at 6 MHz. The fifth section is the same application where the sensing of the common mode of the interferometer is done on the light reflected by the interferometer (photodiode D2), demodulated at 18 MHz.

This note considers the last stage of frequency stabilisation alone. Its interaction with other servo loops has to be considered in a forthcoming note. Some topologies may induce some other requirements on laser frequency noise (see for example [3]) in the low frequency range. This issue will not be discussed since it depends on the topology of the various servo loops used to lock the interferometer. The issues related to lock acquisition (for example transients) will not be discussed either.

[1] Contrary to what is sometimes thought, the laser frequency reference is not the recycling cavity length, but the average of the lengths of the two 3 km arms.

2 Calculation of the transfer functions with the JAJY program

2.1 Principles and setup of the JAJY program

2.1.1 Description of JAJY

JAJY, written by J.-A. Marck and J.-Y. Vinet, is a frequency domain model of the full interferometer. Its principles are described in the chapter 6, "Modulation and transfer functions", of [4]. The mathematical description of JAJY is necessary to stand the case of non negligeable modulation index and to compute the response of the interferometer at frequencies close to or higher than the long arm free spectral range.

The parameters used in the simulation are the following: each long Fabry-Perot cavity is 2999.9 m long; the recycling cavity is 12.053 m long, the optical length difference of the Michelson part (between the west and north mirrors) is 0.878 m. The finesse asymmetry of the long Fabry-Perot cavities is 5 %, the average being 50 (so that the two finesses are 51.25 and 48.75). The end mirrors of the long arm have a zero transmission. The recycling mirror reflects 92% of the incident light power. Each mirror has a loss coefficient of 20 ppm. The AR face of the beamsplitter reflects 500 ppm of the power. The dark current of each photodiode is set to zero. The laser input power is 20 W.

In a complicated optical object like the Virgo interferometer, one should be careful at the definition of the demodulation phases: for example, on the dark fringe port, the carrier and the sidebands have experienced different dephasing so that the definition of "phase" and "quadrature" is not obvious. The JAJY program defines the "quadrature" of the dark fringe port (D1) so that it optimizes the signal-to-noise ratio at 100 Hz, the signal being the gravitational wave strain, the noise being the shot noise. The "phase" on D1 is such that the demodulation sinewave adds a $\pi/2$ angle. The "phase" on D2 and D5 optimizes the signal-to-noise ratio at 100 Hz, the signal being a frequency noise and the noise the shot noise. The "quadrature" on D2 and D5 adds a $\pi/2$ angle to the demodulation sinewave. It can be checked that the "quadrature" of D1 optimizes also the response to laser frequency noise.

In the "quadrature" of D1, and "phase" of D2 and D5, it can be checked that optimizing the signal-to-noise ratio at 100 Hz leads to demodulation phase angles very close to the ones that maximize the signal size (and also the shot noise level).

In the "phase" of D1, and "quadrature" of D2 and D5, the exact tuning of the demodulation angles can produce big changes on transfer functions amplitudes and phases, since the extinction of the defined signal varies a lot. It is not an issue for the transfer function considered in this note, since these transfer functions are not used.

The behaviour of the interferometer to either laser frequency noise or gravitational wave strain is not obvious for frequencies close to the free spectral range of the long arms. Contrary to their use in a Fabry-Perot, the sidebands are not stable references : they experience a recycling gain (35.6) slightly different from the one of the carrier (46.5). The sidebands experience both amplitude and phase change when detuned by a few 100's of Hz.

The JAJY programs first tunes the various cavities. The long Fabry-Perot are brought to resonance. The dark fringe is tuned so that the Michelson has a maximum reflection for the carrier, but due to the length asymmetry, the sidebands are partly transmitted. The recycling cavity is tuned to have maximum gain for the carrier. Then JAJY optimizes the modulation frequency and the modulation index so that gravitational wave to shot noise ratio is maximum on the quadrature of D1. Then, it optimizes the demodulation phase to maximize the same signal to noise ratio at 100 Hz. Then, it computes the optimal demodulation angles on D2 and D5, for maximizing their response to a laser frequency noise. Then a transfer function, between either gravitational wave or laser frequency noise, and the demodulated and filtered current on the photodiode is computed. The −6 dB of the mixer, in the demodulation process, is taken into account.

The calculation of the shot noise in JAJY takes into account the fact that the noise is non stationary (cf. [4]). It can be checked that optimizing the signal to noise ratio maximizes also the noise level. The discrepancy with the calculation that takes into account only the DC current is particularly important on the D1 photodiode, due to the fact that the laser power on this photodiode is mainly due to the sidebands.

2.1.2 Comparison with a Matlab model

The JAJY program transfer functions, if the "signal" is the laser frequency noise, can be checked with the transfer functions computed by the "STF" program [5]. The comparison has been successful, both in the transfer functions phases and amplitudes (in W/Hz). Due to the definition of the Fourier transform used by JAJY model, the complex conjugate should be taken before any use of transfer functions. The transfer functions show slight mismatches for "quadrature" in D2 and D5 and "phase" in D1, due to small mismatching of demodulation angles (of the order of 1 mrad) leading to different extinctions of the signal.

2.1.3 Comparison with experimental data

The low frequency response of JAJY in the case of a simple Fabry-Perot cavity matches the well known Pound-Drever-Hall signal amplitude and shape. The response of a single Fabry-Perot cavity at f being equal to the free spectral range seems also to match the experimental data [6, 7].

2.1.4 First results of JAJY

With the parameters above, the best modulation frequencies are 6.263415 MHz and 18.659996 MHz, the modulation indices being 0.0661 and 0.0549.

For the 6.26 MHz modulation frequency, JAJY gives the following results, where $\theta_{\nu\to Di}$ notes the transfer function between frequency noise and demodulated, filtered current on diode Di, and $\theta_{h\to Di}$ notes the transfer function between a gravitational wave strain and demodulated, filtered current on diode Di:

photodiode	D1	D2	D5
DC power (watts)	0.0203	18.3	0.229
phase definition	Q	P	P
demodulation angle(rad)	2.436	0.176	0.977
shot noise (W/$\sqrt{\text{Hz}}$)	7.56×10^{-11}	1.85×10^{-9}	2.07×10^{-10}
$\theta_{\nu\to Di}(DC)$(W/Hz)	-4.55×10^{-4}	0.174	-1.28×10^{-3}
$\theta_{h\to Di}(DC)(W/unit)$	-3.44×10^{12}	6.06×10^{11}	-1.20×10^{10}

For the 18.66 MHz modulation frequency, results are:

photodiode	D1	D2	D5
DC power (watts)	0.0289	18.3	0.229
phase definition	Q	P	P
demodulation angle(rad)	0.695	0.319	2.609
shot noise ($W/\sqrt{Hz}$)	8.99×10^{-11}	1.85×10^{-9}	2.07×10^{-10}
$\theta_{\nu \to Di}(DC)(W/Hz)$	5.41×10^{-4}	4.04×10^{-2}	-5.18×10^{-4}
$\theta_{h \to Di}(DC)(W/unit)$	4.10×10^{12}	1.41×10^{11}	-4.84×10^{9}

Since

$$D1_Q = \alpha(h + \beta\frac{\delta\tilde{\nu}}{\nu_0}) \tag{3}$$

The effective β asymmetry can be compared with $\beta_{\mathcal{F}}$, the finesse asymmetry:

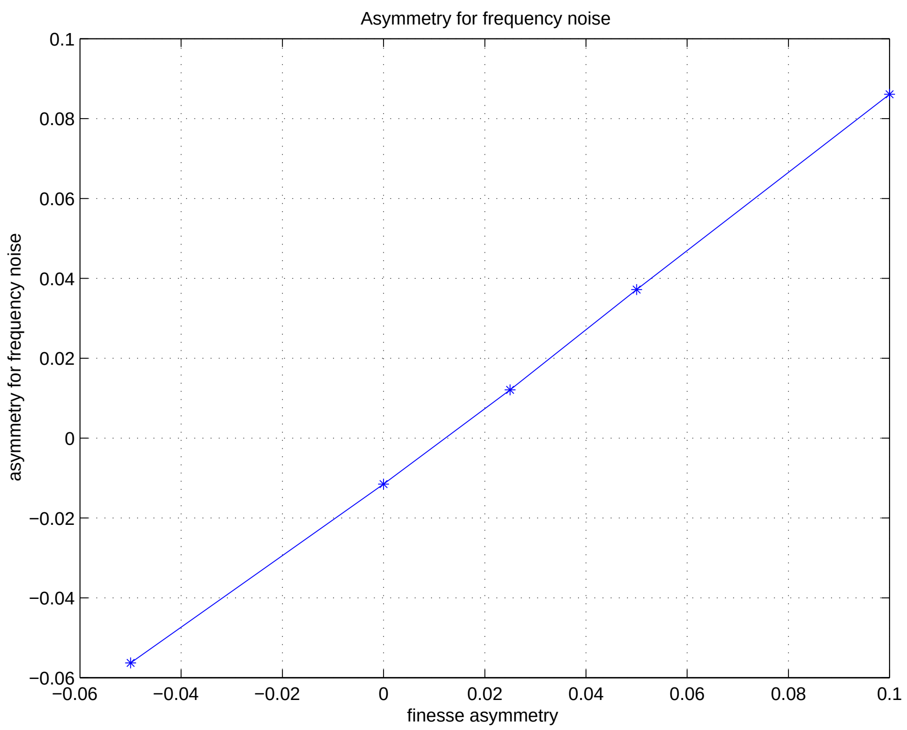

Figure 1: Effective asymmetry for frequency noise versus finesse asymmetry

From the figure 1, it is clear that the effective finesse is proportional to the finesse asymmetry, with an offset of 1.15 %, so that with a finesse asymmetry of 5 %, the effective asymmetry for frequency noise is 3.7 %.

2.2 Calculation of the laser frequency noise requirement

A simplified representation of the interferometer as concerns the laser frequency noise and stabilisation is:

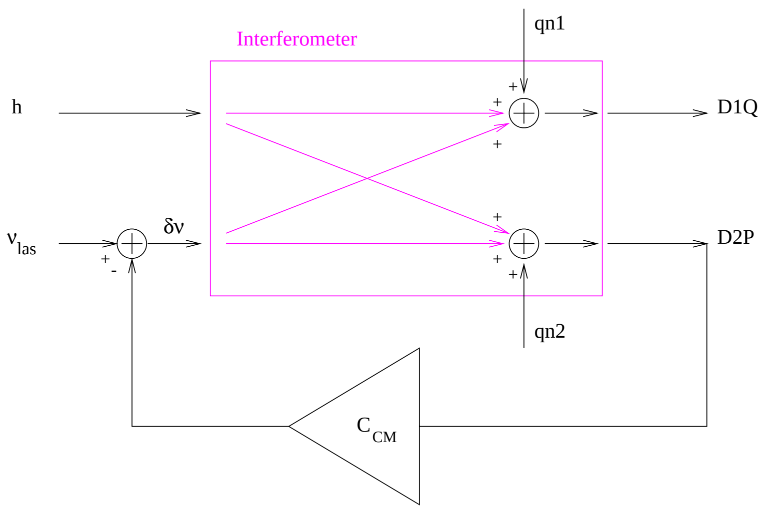

Figure 2: Model of the interferometer as concerns the laser frequency stabilisation and noise

In figure 2, the interferometer is described by two main input ports (gravitational wave strain and laser frequency noise) and two output ports, photodiodes D1 and D2. Four transfer functions are involved between laser frequency noise or gravitational wave strain and demodulated, filtered current on photodiodes D2 (in phase) and photodiode D1 (in quadrature). The q_{n1} and q_{n2} inputs represent the shot noise levels on the corresponding ports, for the optimized demodulating phases. The signal on photodiode D2 is fedback to the laser via the "common mode" corrector filter $C_{\rm CM}$, so that the pre-stabilized laser frequency noise $\nu_{\rm las}$ is reduced to the stabilized laser frequency noise δ_ν.

The open loop transfer function for the laser frequency stabilisation is:

$$G_{\rm CM} = C_{\rm CM}\theta_{\nu\to D2} \tag{4}$$

Simple alegra leads to:

$$s_{\rm D1} = \frac{\theta_{\nu\to D1}}{1+G_{\rm CM}}\left(\nu_{\rm las} + (1+G_{\rm CM})\frac{\theta_{h\to D1}}{\theta_{\nu\to D1}}(1-\kappa)h_{TN} + \frac{1+G_{\rm CM}}{\theta_{\nu\to D1}}q_{n1} - \frac{G_{\rm CM}}{\theta_{\nu\to D2}}q_{n2}\right) \tag{5}$$

where

$$\kappa = \frac{G_{\rm CM}}{1+G_{\rm CM}}\frac{\theta_{h\to D2}}{\theta_{h\to D1}}\frac{\theta_{\nu\to D1}}{\theta_{\nu\to D2}} \tag{6}$$

and h_{TN} is the thermal noise limit of the sensitivity of the interferometer, as described in [8].

If one uses the D5 photodiode instead of the D2 photodiode, all "2" subscripts should be switched to "5" subscripts.

So that the requirement on the prestabilized laser frequency noise is:

- $$|\nu_{\rm las}|^2 < \left|(1+G_{\rm CM})\frac{\theta_{h\to D1}}{\theta_{\nu\to D1}}(1-\kappa)h_{TN}\right|^2 + \left|\frac{1+G_{\rm CM}}{\theta_{\nu\to D1}}q_{n1}\right|^2 \tag{7}$$

- $$\left|\frac{G_{\rm CM}}{\theta_{\nu\to D2}}q_{n2}\right| \ll |\nu_{\rm las}| \tag{8}$$

2.3 Requirements for the stabilized laser frequency noise

One can express the $s_{\rm D1}$ signal as a function of the stabilized laser frequency noise $\delta\nu$, so that the open loop transfer function does not enter into account. One obtain then

$$|\delta\nu| < \left|\frac{\theta_{h\to D1}}{\theta_{\nu\to D1}}(h_{TN} + q_{n1}\frac{1}{\theta_{h\to D1}})\right| \tag{9}$$

If one plots the $(h_{TN} + q_{n1}\frac{1}{\theta_{h\to D1}})$ term, one will obtain a sensitivity curve higher than usual (see for example reference [8]) because the shot noise level on D1 was underestimated, it did not take into account the non-stationarity of the current.

Figure 3: Requirement on the stabilized laser frequency noise, effective asymmetry is 3.7 %, no margin. The pole of the recycling cavity at 10 Hz is naturally taken into account.

3 Design and requirement using D5 photodiode at 6 MHz

3.1 Design of the common mode servo loop

The amplitude of the transfer function between laser frequency noise and demodulated, filtered current on D5 photodiode is:

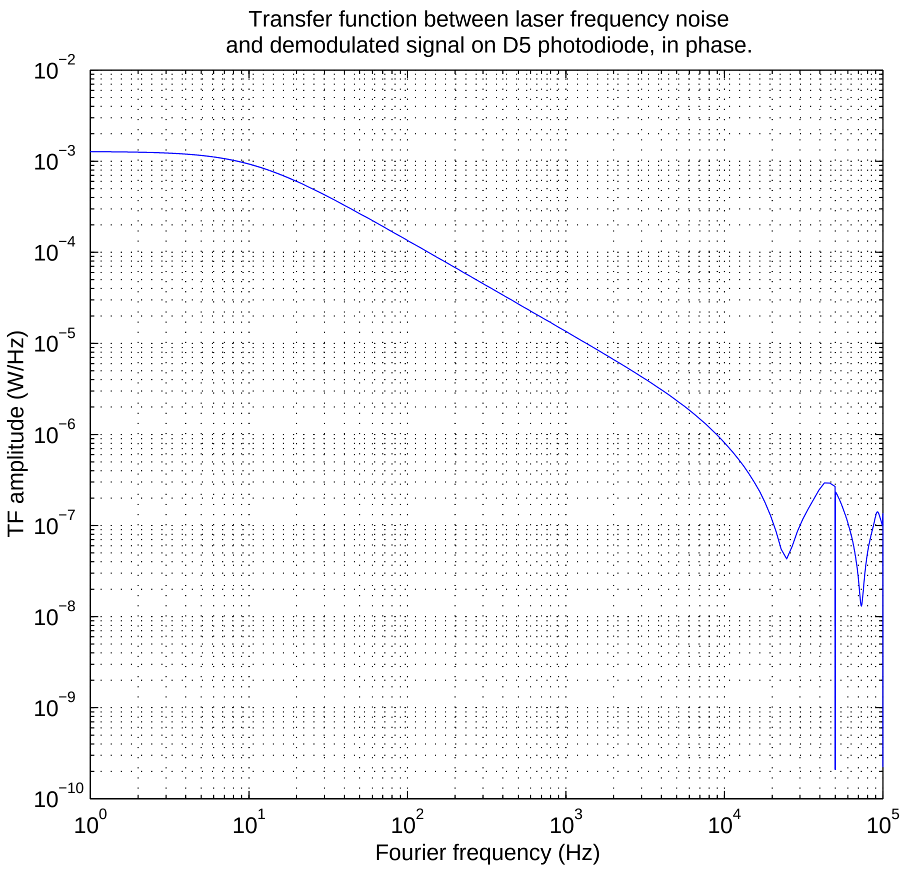

Figure 4: Amplitude of the transfer function.

In the figure 4, one sees the expected pole of the recycling cavity at 10 Hz (see [2] page 36):

$$f_{\mathrm{RC}} = \frac{f_{\mathrm{FP}}}{(1-\zeta_{\mathrm{FP}})\zeta_{\mathrm{FP}}} \frac{(1-\zeta_{\mathrm{RC}})}{G_{\mathrm{RC}}} \tag{10}$$

where $f_{\mathrm{FP}} = 500$ Hz is the pole of the long Fabry-Perot cavity, ζ_{FP} is close to -1 (they are well overcoupled), $\zeta_{\mathrm{RC}} = -0.709$ with the current set of parameters for the carrier (losses in the interferometer are low).

The transfer function has a deep notch at f equal to the free spectral range of the long arm. For frequencies close to half of the free spectral range, the transfer function shows up a notch; actually everything happens as if the transfer function was modulated by a sinewave of period the free spectral range of the long arms. This effect is due to the sidebands in the recycling cavity:

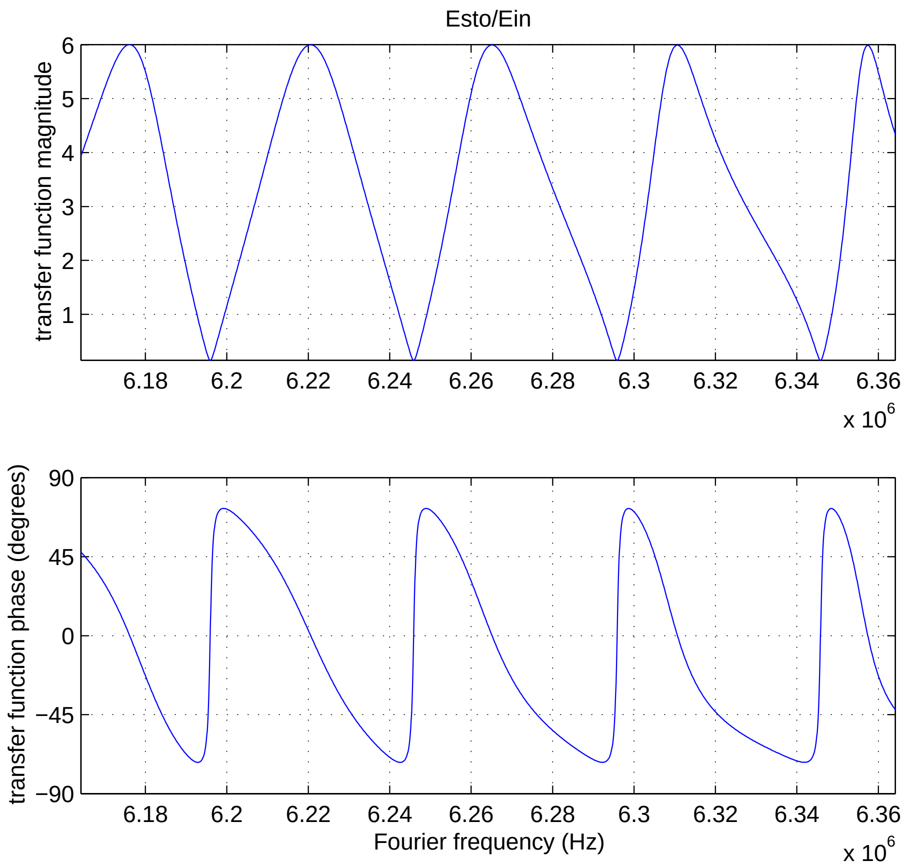

Figure 5: Transfer function between incident electrical field and electrical field inside the recycling cavity, for frequencies around the modulation frequency (computed by Stf).

The light that arrives on the D5 photodiode is the light in the recycling cavity, transmitted through the beamsplitter, reflected on the north arm. One might expect an additional pole at 500 Hz because of the reflection on the north arm; JAJY shows that this is not the case.

A corrector that optimizes open loop unity gain frequency and gain can be:

Poles		Zeroes	
frequency (Hz)	Q	frequency (Hz)	Q
10	5	6000	5
10	5	2000	5
30000	5	40000	5

So that the open loop transfer function, in the Nichols plot, looks like:

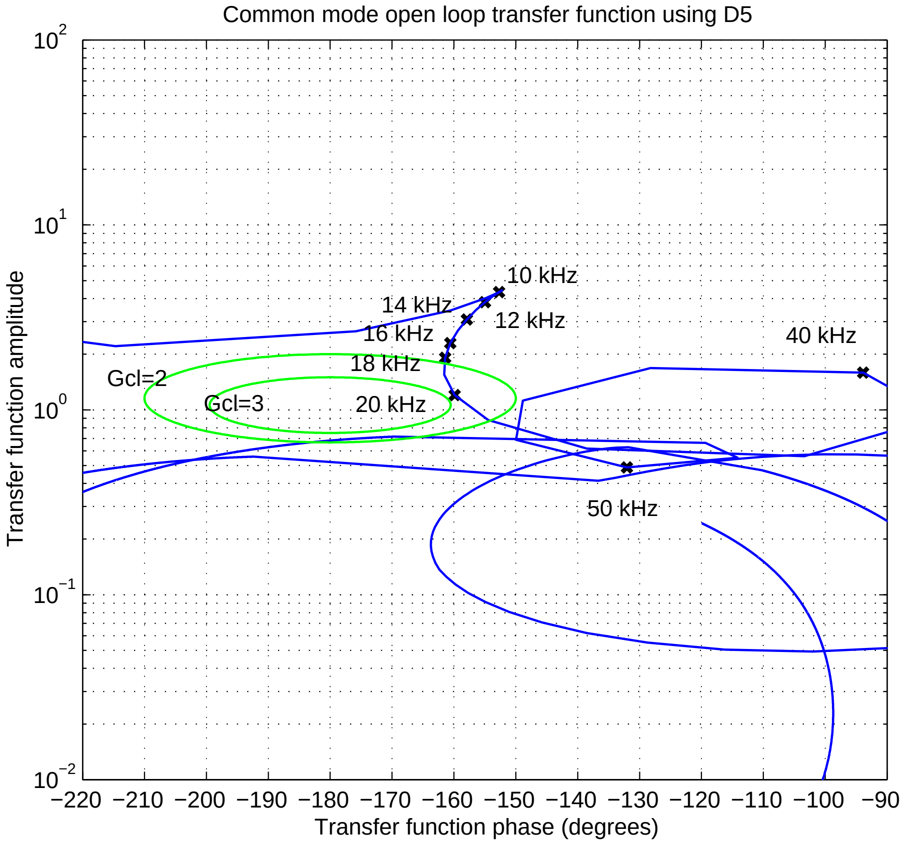

Figure 6: Open loop transfer function, zoom around the unity point. Some selected frequencies are displayed. The two green circles correspond to closed loop gain of 2 and 3.

The unity gain frequency is then 20.5 kHz, the gain margins are +2.5 (increasing)and 1.4 (decreasing), the phase margin is 20°. The bump size in closed loop is a factor of 3 at 20 kHz.

3.2 Requirement on laser frequency noise

Then the requirement on the laser frequency noise at the output of the mode cleaner, as given by equations 7 and 8 are:

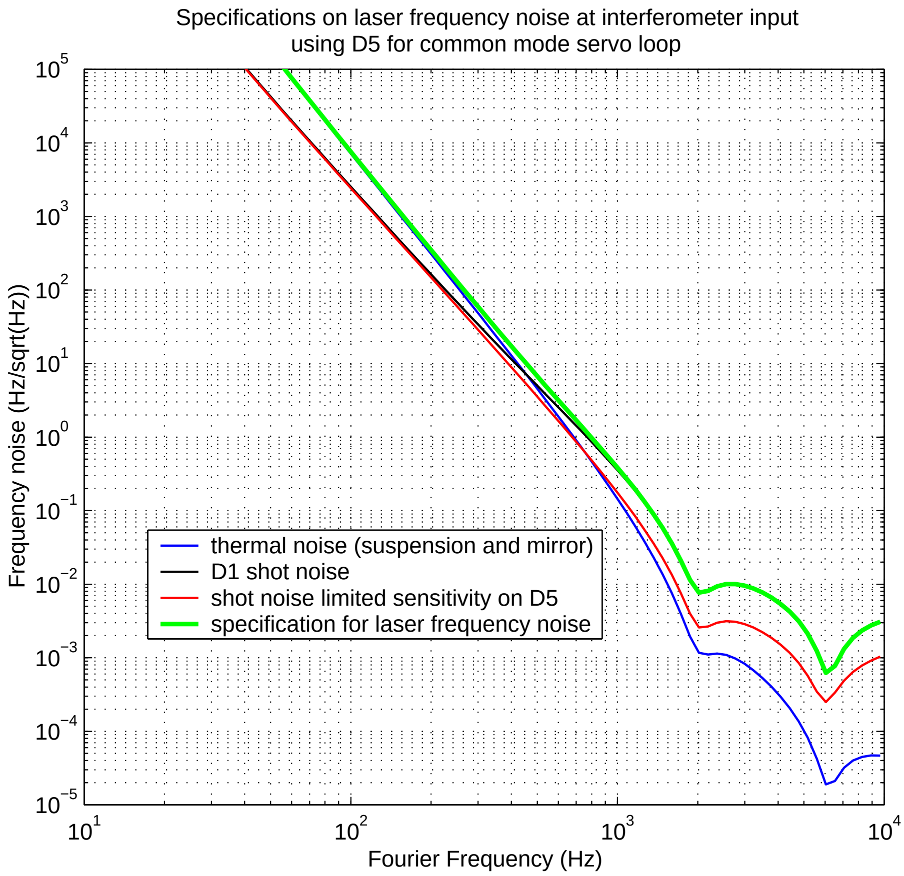

Figure 7: The blue curve is the D1 thermal noise contribution to laser frequency noise, whereas the black one is the D1 shot noise contribution. The green curve is the quadratic sum of these two contributions (blue and black). The red curve is the shot noise sensitivity of D5, using the 230 mW that should arrive on D5.

The laser frequency noise at the output of the mode cleaner should attain a sensitivity of $6 \times 10^{-4}\mathrm{Hz}/\sqrt{\mathrm{Hz}}$ at 6 kHz ($3 \times 10^{-16}\mathrm{m}/\sqrt{\mathrm{Hz}}$). At 200 Hz, the shot noise sensitivity of D5 is only a factor of 2 away from the laser frequency stabilisation goal (without any margin).

4 Design and requirement using D2 photodiode at 6 MHz

4.1 Design of the common mode servo loop

The transfer function between laser frequency noise and demodulated, filtered current on D2 photodiode is:

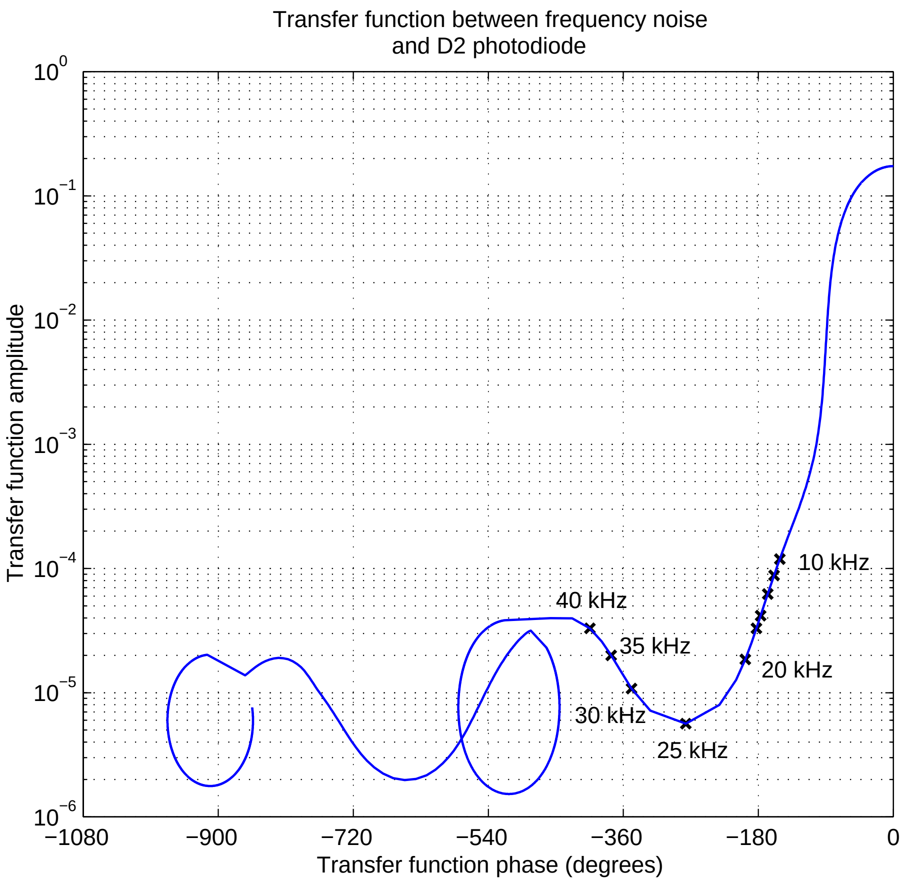

Figure 8: Transfer function between laser frequency noise and demodulated, filtered signal on D2 photodiode.

The $-140°$ dephasing at 10 kHz will make it difficult to obtain a very high unity gain. A corrector that optimizes open loop unity gain frequency and gain can be:

Poles		Zeroes	
frequency (Hz)	Q	frequency (Hz)	Q
10	2	3000	2
10	2	500	2
25000	10		

So that the open loop transfer function, in the Nichols plot, looks like:

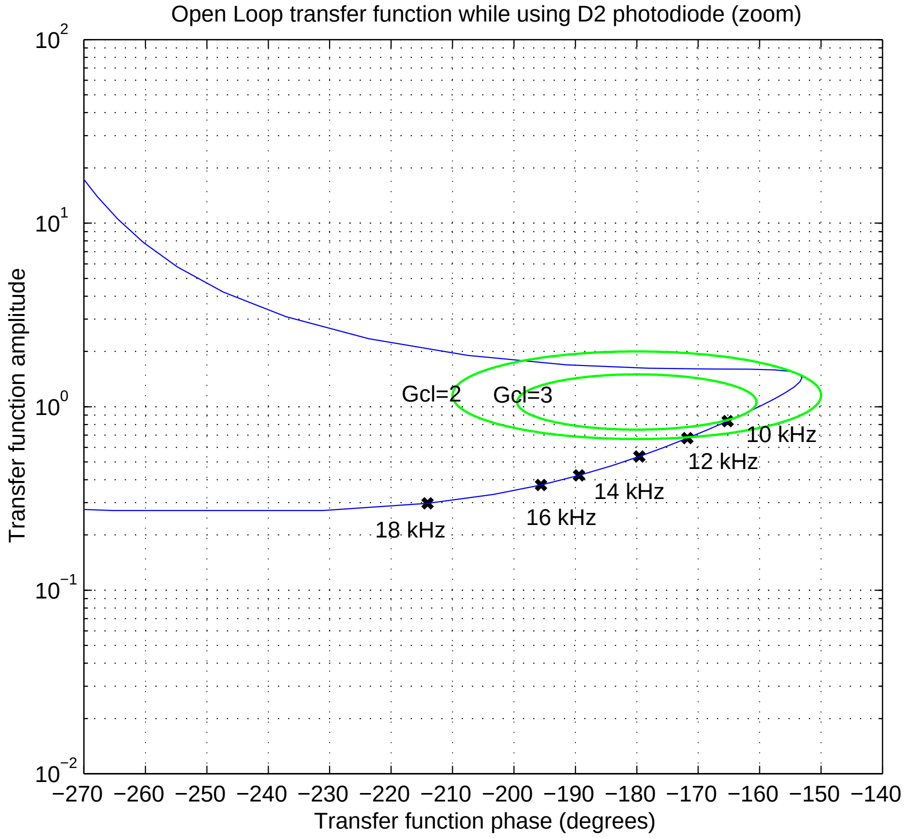

Figure 9: Open loop transfer function, zoom around the unity point. Some selected frequencies are displayed. The two green circles correspond to closed loop gain of 2 and 3.

The unity gain frequency is then 8.35 kHz, the gain margins are +1.6 (increasing)and 2 (decreasing), the phase margin is 20°. The bump size in closed loop is a factor of 3 at 10 kHz.

4.2 Requirement on laser frequency noise

Then the requirement on the laser frequency noise at the output of the mode cleaner, as given by equations 7 and 8 are:

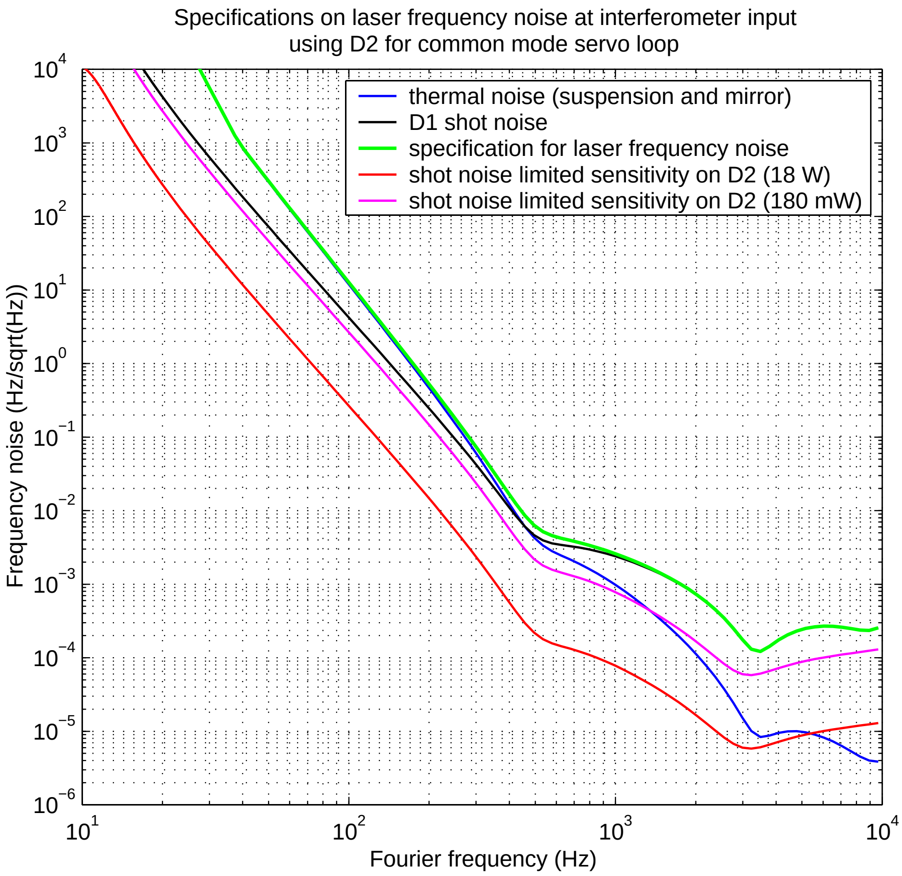

Figure 10: The blue curve is the D1 thermal noise contribution to laser frequency noise, whereas the black one is the D1 shot noise contribution. The green curve is the quadratic sum of these two contributions (blue and black). The red curve is the shot noise sensitivity of D2, using the full 18 W that should arrive on D2.

The laser frequency noise at the output of the mode cleaner should attain a sensitivity of $1 \times 10^{-4}\mathrm{Hz}/\sqrt{\mathrm{Hz}}$ at 3 kHz ($5 \times 10^{-17}\mathrm{m}/\sqrt{\mathrm{Hz}}$). Of course, the reflected power is much to big to fit with the photodiode maximum current (200 mW). With a pick-up of 1 %, the shot noise limit sensitivity of D2 will be then close to the goal.

5 Design and requirement using D2 photodiode at 18 MHz

5.1 Design of the common mode servo loop

When using the 18.66 MHz modulation frequency, the behavior of the transfer function when using the D2 photodiode becomes different. Due to the Michelson length asymmetry, the transmission of the Michelson becomes greater than the transmission of the recycling mirror, so that, for the sidebands, the recycling cavity appears as under-coupled. The reflected field versus incident field transfer function does not experience dephasing anymore for the sidebands, so that the global transfer function has a nice looking :

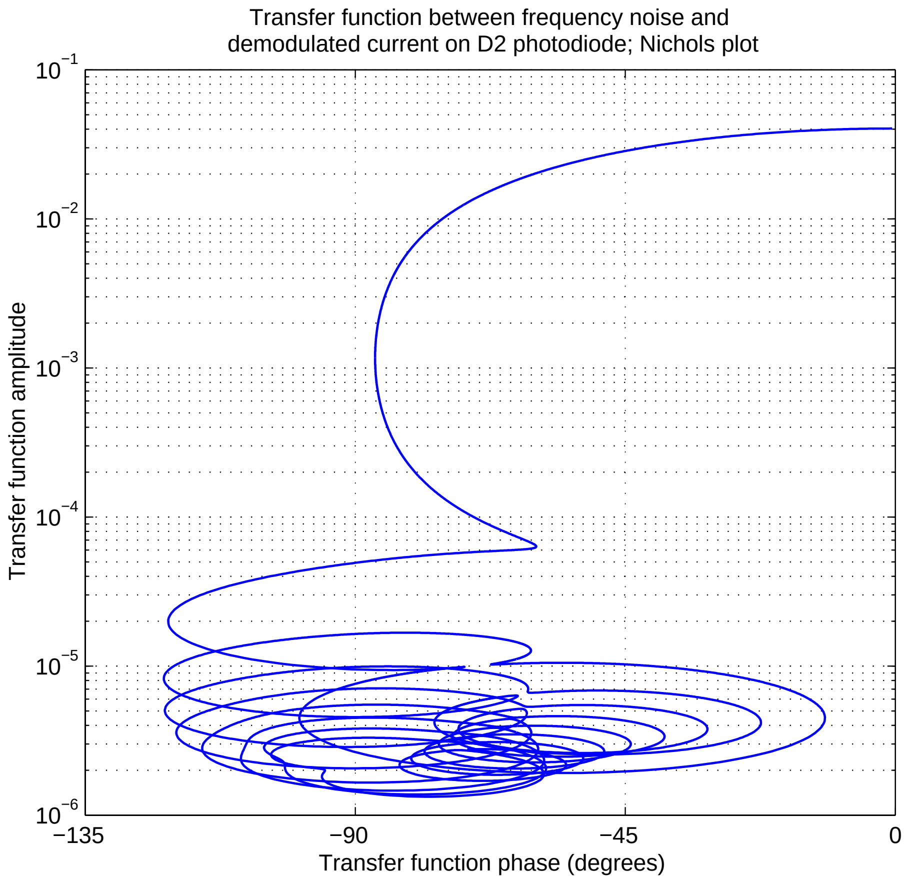

Figure 11: Transfer function for D2 photodiode up to 400 kHz. No crossing of the 180° at f multiple of FSR.

There is plenty of phase margin, so it is possible to build a loop with very high unity gain.

A possible corrector is:

Poles		Zeroes	
frequency (Hz)	Q	frequency (Hz)	Q
10	2	30000	2
10	2	20000	2
400000	0		

A quality factor of 0 means a simple pole in this table.

Then the open loop transfer function, in the Bode plot, is:

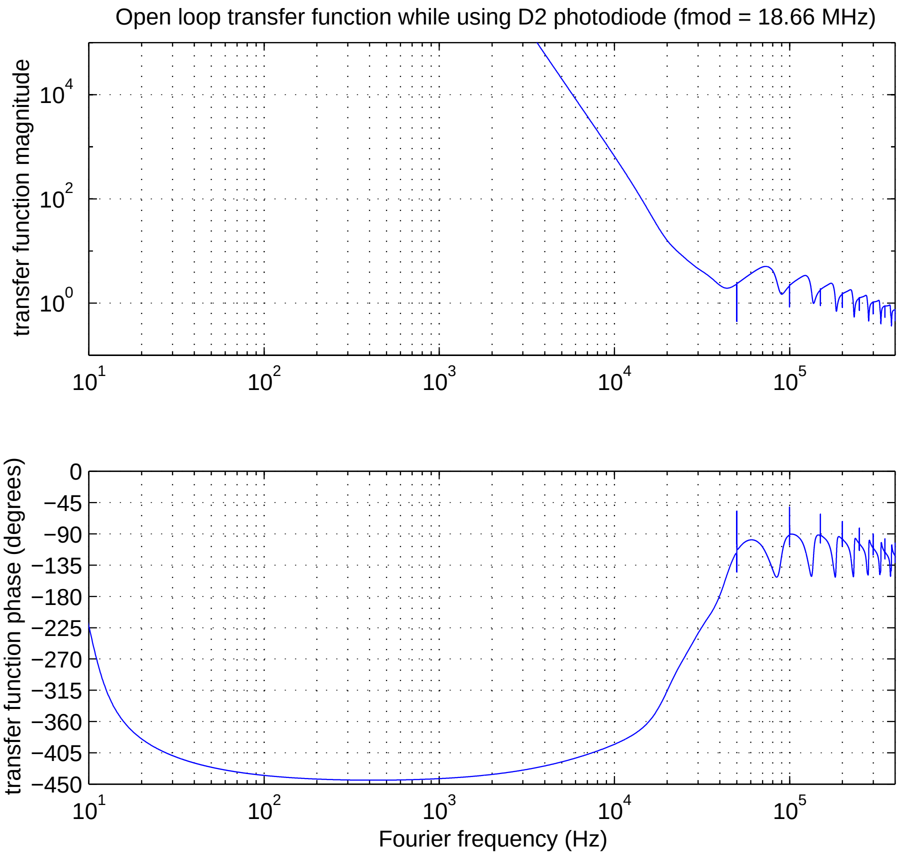

Figure 12: Open loop transfer function when using the D2 photodiodes

The unity gain is approximately 250 kHz (the unity gain is crossed several times). Phase margin is 30° and gain margin is 2.

5.2 Requirement on laser frequency noise

The loop gain at 10 kHz is about 1000, so the requirement on the laser frequency noise is much easier to obtain:

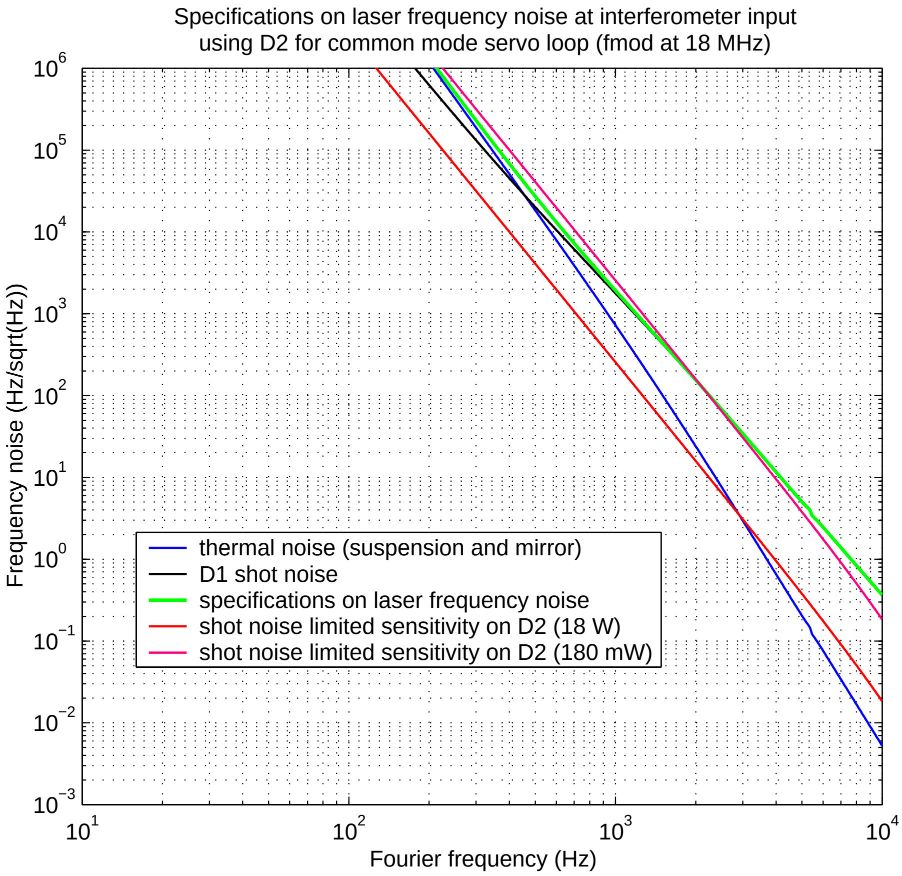

Figure 13: The blue curve is the D1 thermal noise contribution to laser frequency noise, whereas the black one is the D1 shot noise contribution. The green curve is the quadratic sum of these two contributions (blue and black). The red curve is the shot noise sensitivity of D2, using the full 18 W that should arrive on D2.

The problem of the big power arriving on D2 is the same : a pick-up mirror will have to be used if the losses in the interferometer are low, and the shot noise sensitivity of D2 will become close to the specification.

6 Discussion

6.1 About the interferometer model

The figure 2 is a simplified one. The conversion from thermal noise to h sensitivity is not exactly a number, but a transfer function. Since the thermal noise is visible up to 500 Hz, the approximation is good anyway. But some thermal noise may also limit the measurement resolution on the D2 or D5 photodiodes. A model that takes all inputs into account is:

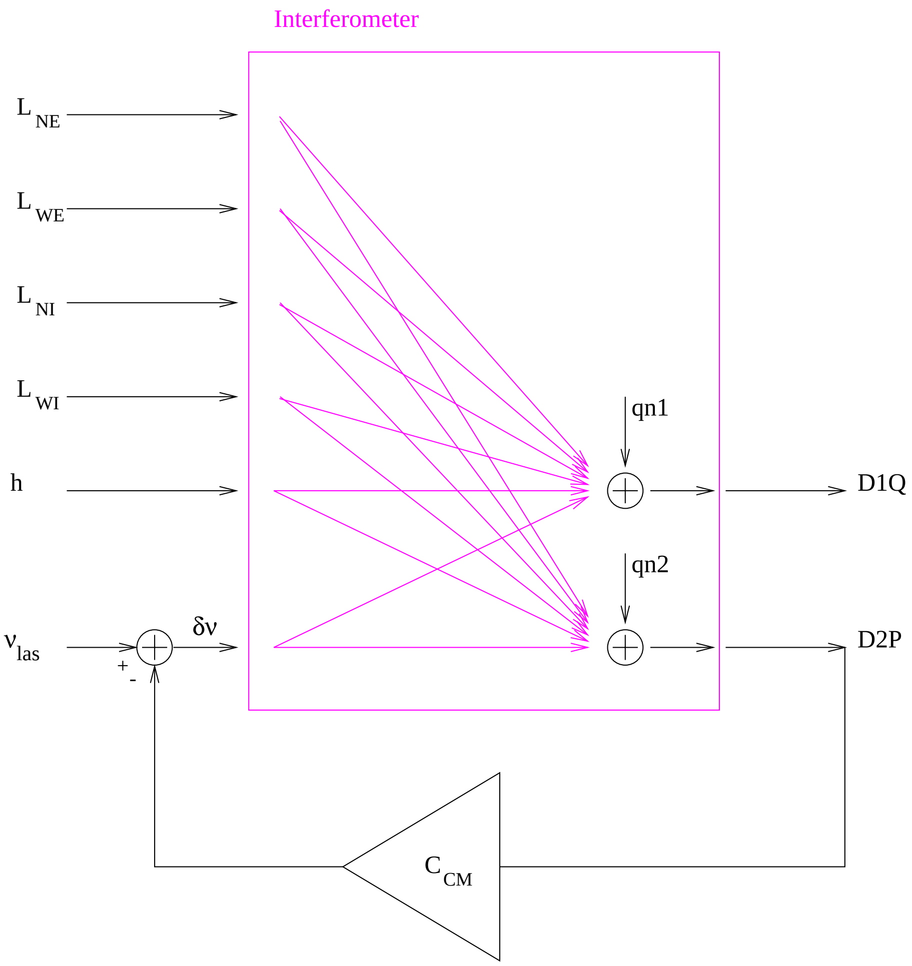

Figure 14: The interferometer has actually six main inputs: the four test masses, the gravitational wave strain and the laser frequency noise. There are transfer functions between all these inputs and the dark fringe and the channel used to stabilize the laser frequency.

The signal on the dark fringe is then:

$$s_{\mathrm{D1}} = \frac{\theta_{\nu\rightarrow D1}}{1+G_{\mathrm{CM}}}\nu_{\mathrm{las}} + \theta_{h\rightarrow D1}(1-\kappa_h)h + \theta_{Mi\rightarrow D1}(1-\kappa_{Mi})l_i + q_{n1} - \frac{G_{\mathrm{CM}}}{1+G_{\mathrm{CM}}}\frac{\theta_{\nu\rightarrow D1}}{\theta_{\nu\rightarrow D2}}q_{n2} \qquad (11)$$

where $\theta_{Mi\rightarrow D1}(1-\kappa_{Mi})l_i$ is actually a sum on all four test masses, $\theta_{Mi\rightarrow D1}$ being $\theta_{NI\rightarrow D1}$ for the NI (north-input) mirror, $\theta_{WI\rightarrow D1}$ for the WI (west-input) mirror, $\theta_{NE\rightarrow D1}$ for the NE (north-end) mirror, and $\theta_{WE\to D1}$ for the WE (west-end) mirror. κ_{Mi} is defined by:

$$\kappa_{Mi} = \frac{G_{\rm CM}}{1+G_{\rm CM}} \frac{\theta_{\nu\to D1}}{\theta_{\nu\to D2}} \frac{\theta_{Mi\to D2}}{\theta_{Mi\to D1}} \quad (12)$$

It is possible to check with JAJY that each κ_{MI} is much smaller than one at all frequencies, even at f=FSR.

It must be noted that $\theta_{h\to D1}$ is not exactly equal to $(-l_{NI}+l_{WI}+l_{NE}-l_{NW})/L_{\rm arm}$. Actually, each $\theta_{Mi\to D1}$ is slightly different by a few percent, as well as the sum.

On the contrary, $\theta_{\nu\to D2}$ is very close in DC (0.04% difference) to $(-l_{NI}+l_{WI}-l_{NE}+l_{NW})\nu_0/2L_{\rm arm}$, even if each individual transfer function differ from the others by a few percent. But the transfer functions have different poles, so the frequency response is differs: $\theta_{\nu\to D2}$ shows a pole at 10 Hz (and some more structure above 20 kHz), while $\theta_{l_+\to D2}$ displays a pole at 10 Hz and a zero at 500 Hz. But then the thermal noise contribution becomes negligible, so that the result is left unchanged (the κ_{Mi} are smaller than unity).

So the simplified model gives accurate numbers, at least up to a few percent.

6.2 transfer functions and parameter variation

The transfer function $\theta_{\nu\to D2}$ is left almost unchanged (variation less than a percent in amplitude and a few degrees in phase) while varying the modulation frequency by 500 Hz, the demodulation phase on D2 by 0.1 radian, the modulation index by 10 %, and the asymmetry changed from + 5 % to - 5 %. The biggest change comes from the change of loss level from 20 to 100 ppm per mirror, where the phase delay at 10 kHz is increased by 10 degrees.

The transfer function $\theta_{\nu\to D5}$ seems to be not sensitive to changed losses on the mirrors.

7 Conclusions

I have studied the different possibilities for the last stage of frequency stabilisation in Virgo and designed the correction filter to be used in different cases.

I propose that we use the signal on the D5 photodiode (demodulated at 6.22 MHz) to control the laser frequency fluctuations. This allows a larger unity gain frequency than the D2 photodiode, and reduces the requirements on the prestabilisation. I recommend anyway to design the frequency control system with enough flexibility, in order to allow for the use of different filters.

Increasing the finesse of the long arms would improve the filtering of the laser noise. In addition, the impedance matching would also be improved by increasing the finesse of the recycling cavity. That would improve both the sensitivity of Virgo and the shot noise in the frequency control loop. It requires the replacement of the initial PR mirror by a more reflective one; this improvement could take place after the measurement of the actual interferometer losses.

There is some introduction of the shot noise of photodiode D2 (or D5) on the dark fringe via the laser frequency stabilisation. The only way to cancel that effect is to improve the symmetrisation of the interferometer.

This study also shows that the frequency control loop would be much more effective if the modulation frequency was higher (18.66 MHz), but this advantage would be partially cancelled by the improvement of the impedance matching and requires taking into account some other technical problems, like the noise of the input mode cleaner.

References

[1] C.N. Man and A. Brillet. Update on the requirements of the laser frequency prestabilization. Virgo note PJT 94036, 1994.

[2] F. Bondu. *Étude du bruit thermique et stabilisation en fréquence du laser du détecteur interférométrique d'ondes gravitationnelles VIRGO.* PhD thesis, Université Paris XI (Orsay), 1996.

[3] M. Barsuglia. *Stabilisation en Fréquence du laser et contrôle de cavités optiques à miroirs suspendus pour le détecteur interférométrique d'ondes gravitationnelles VIRGO.* PhD thesis, Université Paris XI (Orsay), 1999.

[4] The Virgo collaboration. The virgo physics book, vol. ii, optics and related topics. /www.virgo.infn.it/, documents, virgo physics book, vol. II., March 2002.

[5] F. Bondu. Simulation of transfer functions of virgo using matlab. /virgoDev/Stf, 2001. see /virgoDev/Stf/SimOptTF.htm for documentation.

[6] R. Savage. Measures on the ligo 4 km x arm. Personal communication, November 2002.

[7] F. Bondu. Measures on the virgo input mode cleaner, May 2001.

[8] G. Cagnoli, L. Gammaitoni, and J. Kovalik et al. The virgo sensitivity curve. Virgo Note VIR-NOT-PER-1390-51, 1999.

[9] R. Flaminio. Talk at Orsay, 1995.